RESEARCH ARTICLE

Key Points:
- Forest-to-atmosphere flux indicated a small C source, 0.7 Mg C ha^{-1} yr^{-1}
- Forest-to-river and water-to-atmosphere fluxes were 0.3 and 0.09-0.14 Mg C ha^{-1} yr^{-1}, respectively
- Fluvial C loss was highest during wet season, especially in the case of DOC

Fluvial carbon export from a lowland Amazonian rainforest in relation to atmospheric fluxes

Leena E. Vihermaa[1], Susan Waldron[1], Tomas Domingues[2], John Grace[3], Eric G. Cosio[4], Fabian Limonchi[4], Chris Hopkinson[5], Humberto Ribeiro da Rocha[6], and Emanuel Gloor[7]

[1]School of Geographical and Earth Sciences, University of Glasgow, Glasgow, UK, [2]Faculdade de Filosofia, Ciências e Letras de Ribeirão Preto, Universidade de São Paulo, São Paulo, Brazil, [3]School of GeoSciences, University of Edinburgh, Edinburgh, UK, [4]Sección Quimica, Pontificia Universidad Católica del Perú, Lima, Peru, [5]Department of Geography, University of Lethbridge, Lethbridge, Alberta, Canada, [6]Instituto de Astronomia, Geofísica e Ciências Atmosféricas, Universidade de São Paulo, São Paulo, Brazil, [7]School of Geography, University of Leeds, Leeds, UK

Abstract We constructed a whole carbon budget for a catchment in the Western Amazon Basin, combining drainage water analyses with eddy covariance (EC) measured terrestrial CO_2 fluxes. As fluvial C export can represent permanent C export it must be included in assessments of whole site C balance, but it is rarely done. The footprint area of the flux tower is drained by two small streams (~5–7 km^2) from which we measured the dissolved inorganic carbon (DIC), dissolved organic carbon (DOC), particulate organic carbon (POC) export, and CO_2 efflux. The EC measurements showed the site C balance to be +0.7 ± 9.7 Mg C ha^{-1} yr^{-1} (a source to the atmosphere) and fluvial export was 0.3 ± 0.04 Mg C ha^{-1} yr^{-1}. Of the total fluvial loss 34% was DIC, 37% DOC, and 29% POC. The wet season was most important for fluvial C export. There was a large uncertainty associated with the EC results and with previous biomass plot studies (−0.5 ± 4.1 Mg C ha^{-1} yr^{-1}); hence, it cannot be concluded with certainty whether the site is C sink or source. The fluvial export corresponds to only 3–7% of the uncertainty related to the site C balance; thus, other factors need to be considered to reduce the uncertainty and refine the estimated C balance. However, stream C export is significant, especially for almost neutral sites where fluvial loss may determine the direction of the site C balance. The fate of C downstream then dictates the overall climate impact of fluvial export.

1. Introduction

Tropical forests cover a vast area, variously estimated at between 17 and 25 × 10^6 km^2 [*Achard et al.*, 2002; *Grace et al.*, 2014]. They exchange energy, mass, and momentum with the atmosphere, and so have the capacity to influence the climate system, locally and regionally [*Costa and Foley*, 2000; *Lean and Warrilow*, 1989; *Shukla et al.*, 1990; *Werth and Avissar*, 2002]. Of particular interest is the exchange of CO_2 with the atmosphere, and the capacity of the forest to act as a store of carbon and a carbon "sink," thus providing a valuable global environmental service by absorbing anthropogenic CO_2 emissions [*Gibbs et al.*, 2007]. Our understanding of how the metabolism of tropical forests determines carbon fluxes, and how underlying processes are influenced by climatological phenomena such as drought, has developed rapidly as a result of (i) measurements and experimentation on trees at the scale of 1 ha plots [*Costa and Foley*, 2000; *Lewis et al.*, 2009; *Lola da Costa et al.*, 2010; *Nepstad et al.*, 2007; *Phillips et al.*, 1998, 2010], (ii) micrometeorological observations at the ecosystem scale using eddy covariance [*Araujo et al.*, 2002; *Carswell et al.*, 2002; *Kruijt et al.*, 2004; *Saleska et al.*, 2009], and (iii) observations at the landscape scale from aircraft-based measurements of atmospheric concentrations of CO_2 [*Chou et al.*, 2002; *Gatti et al.*, 2010, 2014; *Lloyd et al.*, 2007] or lidar-based assessment of standing biomass [*Marvin et al.*, 2014].

Many of the ecosystem studies use eddy covariance to measure the vertical exchange of CO_2 and apportion this to photosynthetic and respiratory processes. Yet there is lateral transport of dissolved and particulate carbon away from the forest in the drainage water, and hence, a strong likelihood of overestimating the terrestrial carbon sink if the C leakage in drainage water is not accounted for [*Richey et al.*, 2002; *Waterloo et al.*, 2006]. For a given site any carbon transported downstream in drainage water constitutes a permanent loss of carbon.

The drainage fluxes comprise dissolved inorganic carbon (DIC), dissolved organic carbon (DOC), particulate organic carbon (POC), and also CO_2 efflux from the river surface. In the Amazon Basin, despite the large EC

network, only at a single site has organic C export been related to EC results [*Monteiro et al.*, 2014; *Waterloo et al.*, 2006]. The fluvial CO_2 efflux, if taking place within a tower footprint, will be captured within the EC measurements, but this CO_2 pool represents a different pathway of carbon movement, distinct from ecosystem respiration, and is required to understand and model the system behavior in detail. For understanding wider ecosystem functioning, the type and processing of the exported C is also important. DOC may be decomposed to CO_2 and lost to the atmosphere along with CO_2 derived from soil respiration. POC may undergo decomposition, be deposited on floodplains, or ultimately, any fraction that has escaped decomposition may be buried in ocean sediments. Deep-sea burial of ecosystem-derived POC will contribute to removal of atmospheric CO_2 [*Galy et al.*, 2015, *Hilton*, 2016].

Understanding the nature of this lateral flux independently of the net carbon balance at a forested site is important. There is a long history of measuring Amazonian aquatic efflux [*Bartlett et al.*, 1990; *Devol et al.*, 1987; *Richey et al.*, 2002], but these measurements have not been combined with eddy covariance measurements. Most recent estimate of the CO_2 emissions from all the rivers and streams (taken as rivers <100 m wide) of the Amazon Basin upstream of Óbidos suggests as much as $0.8 \, \mathrm{Pg \, C \, yr^{-1}}$ is released to the atmosphere [*Rasera et al.*, 2013], far more than is discharged to the ocean at the mouth of the river. A flux of this magnitude is larger than the losses from deforestation and land use change in South America of about $0.5 \, \mathrm{Pg \, C \, yr^{-1}}$ [*Gloor et al.*, 2012] and comparable to fossil fuel burning in the tropics $0.74 \, \mathrm{Pg \, C \, yr^{-1}}$ [*Grace et al.*, 2014] and therefore needs to be considered in any construction of the tropical carbon budget that aims to separate explicitly the different pathways of C movement. The aquatic efflux may also include a contribution of aged carbon, i.e., not recently fixed from the atmosphere by the ecosystem [*Clark et al.*, 2013; *Mayorga et al.*, 2005; *Vihermaa et al.*, 2014]. If it is known that this occurs, a correction for the fraction of fossil carbon inputs must be made for, as otherwise the budget would overestimate the loss of recently fixed C.

The fluxes from forest to drainage water, hereafter called the fluvial export, are likely to vary seasonally according to the hydrological controls. DOC and POC concentrations, [DOC] and [POC], are typically higher in the wet season and during rain events that leach carbon from the forest canopies and soils [*Johnson et al.*, 2006; *Monteiro et al.*, 2014; *Salimon et al.*, 2013; *Townsend-Small et al.*, 2008]. Heavy rain events usually result in a peak [DOC] but the time since previous rain event and the intensity of rain influence this relationship [*Monteiro et al.*, 2014]. DIC concentration, [DIC], has been found to be maximal at low water levels [*Salimon et al.*, 2013; *Sousa et al.*, 2008] with the timing of maximum export flux depending on the balance between the increased discharge and the dilution effect. As the C concentrations and fluxes vary seasonally, according to hydrological controls, quantifying an annual export budget requires data capture over the full hydrological range.

Eddy covariance measurements have not previously been carried out in the Peruvian Amazon where the soils are younger and more fertile in general than the sites studied previously in Brazil. Here we report catchment-scale measurements from a lowland rain forest in Peru in this more fertile area, where forest-to-atmosphere and additionally forest-to-river and river-to-atmosphere fluxes were measured for 1 year during October 2011 to September 2012.

2. Methods

2.1. Study Site

The study site was located in the Tambopata River catchment (latitude 12°49′54.30″S, longitude 69°16′52.37″W), near Puerto Maldonado, Madre de Dios, Peru (Figure 1). It is within the Reserva Nacional de Tambopata, noted for its high biodiversity. For example, a 1 ha plot at the site was found to contain 556 trees in 115 taxa [*Lopez-Gonzalez et al.*, 2012]. The climate is warm and humid. An average annual temperature of 25.4°C and precipitation of 2377 mm was recently reported to be the 112 year average [*Weatherbase*, 2015]. The wind direction is quite variable, with NW as prevailing direction. Elevation gradients of the surface around the flux tower are small (Figure 1), a maximum of 10 m increase in elevation within 0.5 km radius in all directions. The tower footprint has an average daytime area of about 2 km^2 and is covered by 30 m tall primary evergreen forest on soils that vary from well drained to swampy, classed as Haplic Cambisols or Inceptisols in the U.S. Soil Taxonomy [*Quesada et al.*, 2011]. The Tambopata site is part of the more fertile areas within the Amazon Basin, with the soil samples classed in the top 50 percentile of the data in terms of nutrient content in an Amazon Basin-wide soil study [*Quesada et al.*, 2010]. The aboveground biomass in the monitoring plot
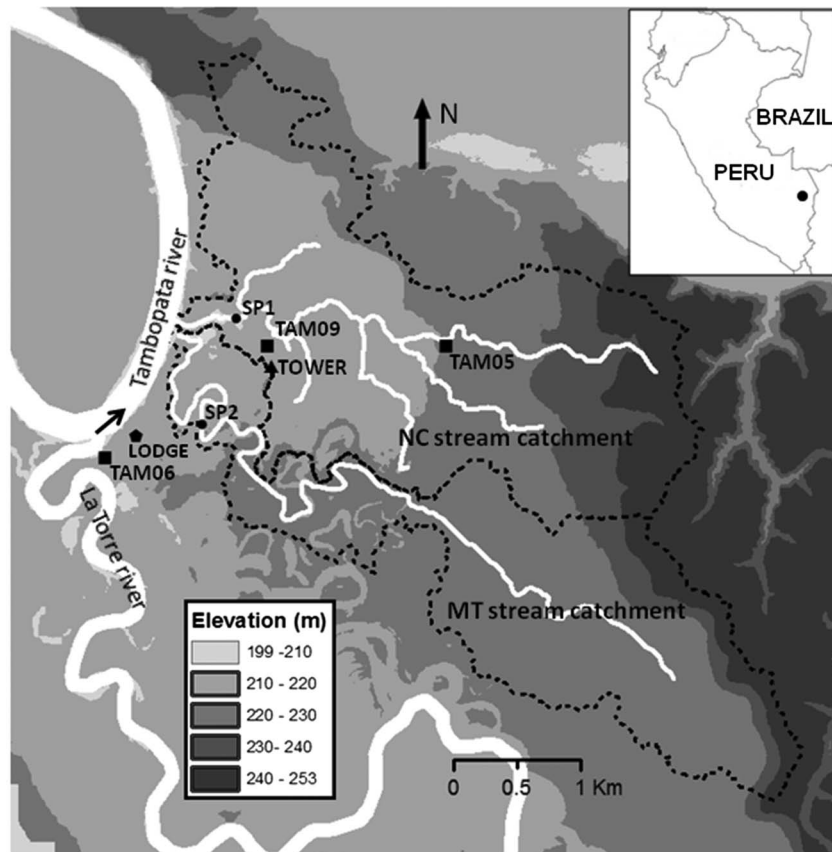
Figure 1. Location of the Ramiro Chacon-SAGES eddy covariance flux tower, the surrounding topography, the two study streams, and the forest biomass sampling plots (TAM5, TAM6, and TAM9) at the Tambopata site. New Colpita is the perennially active Stream 1, and Main Trail is the ephemeral Stream 2. The stream catchment boundaries are marked with dashed line and the sampling points in each system with a dot (SP1 and SP2). Inset: location of the study site in the western part of the Amazon Basin in Madre de Dios region, Peru.

known as TAM09 was 81 Mg C ha^{-1} and 70 Mg C ha^{-1} in the wider forest area surrounding the plot [*Marvin et al.*, 2014]. The selected site is ideal for constructing a detailed C balance as the local forest area is drained only by headwater streams and upstream C inputs do not need to be considered.

2.2. Eddy Covariance Measurements

An eddy covariance flux tower, named "The Ramiro Chacon-SAGES Tower," was constructed in 2010–2011 and flux measurements commenced in September 2011. The tower is a free-standing structure made of 42 m tall steel girders. The instruments for eddy covariance, chosen for their low power consumption, were for CO_2 and H_2O concentration, LI-7200 with a short-path sampling tube and high-flux pump LI-7550 (LI-COR, Lincoln, Nebraska, USA); for CH_4 concentration, LI-7700 (LI-COR, Lincoln, Nebraska, USA); and for wind speed and direction a sonic anemometer, CSAT3 (Campbell Scientific, Utah, USA). Meteorological instruments were solar and thermal radiation, NR01 (Campbell Scientific, Utah, USA); direct and diffuse radiation, BF3 (Delta-T Devices, Burwell, UK); photosynthetically active radiation downwelling and upwelling, LI-190 (LI-COR, Lincoln, Nebraska, USA); temperature and relative humidity, HMP45C (Campbell Scientific, Utah, USA); wind speed and direction, Vector A100P and W 200P (Campbell Scientific, Utah, USA); wetness sensor, SKLW1900 (Skye Instruments, Llandrindod, UK); barometric pressure, CS100 (Campbell Scientific, Utah, USA); and a tipping bucket rain gauge, TB4 (Campbell Scientific, Utah. USA). Air was drawn from above the tower at 15 L min^{-1} via 5.3 mm internal diameter Synflex tube and directed to the CO_2 analyzer. Data for eddy covariance analysis were collected at 10 Hz on a Campbell data logger (CR3000, Campbell Scientific, Utah. USA); for the meteorological data the sensors were scanned every minute. The entire array of instruments runs at around 12 V and 5 A. Power for the instruments was provided by six solar panels: 67 cm × 148 cm, 12 V

nominal, and rated at 42 W each; storage was 560 A h in an array of lead acid batteries mounted at the top of the tower.

Data were filtered to remove cases where the energy balance closure was inadequate due to low wind speed and when the friction velocity ($u*$) value was less than $0.17 \, \mathrm{m \, s^{-1}}$ (based on a plot of night flux versus $u*$). Gaps were filled after fitting curves to the relationship between CO_2 flux and photosynthetically active radiation, following the procedure of *Gilmanov et al.* [2007]. GPP (gross primary productivity) was estimated by subtracting an estimate of dark respiration from the net flux during the daylight hours. Dark respiration in the day was estimated from dark respiration at night by correcting for the warmer day temperatures [*Aubrecht et al.*, 2016; *Stoy et al.*, 2006]. Finally, the monthly and annual total fluxes were derived by accumulating the half-hour values.

From 28 May to 16 June 2012 there was a continuous period of 20 days of missing data in the flux tower rainfall record. This was gap-filled using the data from three nearest SENAMHI [*Servicio Nacional de Meteorología e Hidrología del Perú*, 2014] met stations (Tambopata, Limbani, and Puerto Maldonado; Figure S1 in the supporting information). The estimated missing rainfall (37.8 mm; standard deviation 10.4) was added to the rainfall recorded by the tower in the latter half of June (69.4 mm), yielding a total of 107.2 mm.

2.3. Fluvial Carbon Sampling

Two small streams drain the tower footprint area (Figure 1): one is perennially active (Stream 1, New Colpita), while the other (Stream 2, Main Trail) is active only during the wet season. Surface water samples for measurement of [DIC], [DOC], and [POC] were collected during three field campaigns: February–April 2011, September–December 2011, and March–May 2012. Stream 2 dries up during the dry season; therefore, no samples could be collected during September–November 2011. Different flow conditions were targeted in sampling to understand the hydrological controls on the carbon concentrations and fluxes. DIC samples were collected in pre-acidified (150 µL of concentrated phosphoric acid) evacuated 12 ml Exetainers and the headspace analyzed [*Waldron et al.*, 2014] on Thermo-Fisher-Scientific Gas Bench/Delta V Plus for [DIC]. DOC samples were filtered through pre-furnaced (8 h at 450°C) 0.7 µm glass fiber filter paper on the day of sampling and stored refrigerated. Samples treated this way show little change in composition over 3 months [*Gulliver et al.*, 2010]. Prior to the measurement of [DOC] by combustion (Thermalox TOC 2020, Analytical Sciences) the samples were acidified to pH 3.9 and degassed to remove any DIC. [POC] was measured by loss on ignition (LOI) on the filter papers. In this method oven dry (3 h at 105°C) weight was compared to the weight after furnacing (16 h at 375°C). The OC content of the mass loss was assumed to be 50% [*Atjay et al.*, 1977; *Pregitzer and Euskirchen*, 2004], which corresponds well with the measured range C content (45–53%) of different litterfall fractions from the southern Amazon forest but was higher than the fraction (43%) found in coarse POM [*Selva et al.*, 2007]. To assess C inputs in rainfall, [DIC], [DOC], and [POC] were also measured in a limited number of rain water samples collected on the 2012 campaign. The delivery per land area was calculated using rainfall volume-weighted mean concentration of C fractions and the annual total rainfall.

Direct measurements of CO_2 efflux from water surfaces were carried out using a floating chamber connected to a CO_2 analyzer (Li-840A, LI-COR, Lincoln, Nebraska, USA). CO_2 accumulation in the floating chamber head space was measured every second for 4 min, the measurement repeated three times, and the flux rates calculated according to *Frankignoulle* [1988]. Additional water flow velocity measurements (Hand held flow meter, Geopacks, Hatherleigh, UK) were taken in the exact location where the chamber was deployed. A limited number ($n = 4$) of CO_2 efflux measurements were carried out in the flooded forest.

2.4. Stream Catchment Analysis

The streams were mapped by walking along them while recording the route with a hand-held GPS. The stream catchment areas were analyzed in ArcGIS 10 (ESRI, USA) using a digital elevation model (DEM) constructed from lidar data [*Boyd et al.*, 2013; *Hill et al.*, 2011]. Lidar DEM-based stream location data was compared to the field measurements, and good agreement was found. The lidar data allowed analysis of the larger area of the catchment than had been possible to map in the field due to difficulty in cutting routes through the dense vegetation. Upstream of the sampling point, Stream 1, New Colpita, drains an area of 7.2 km², and the seasonal Stream 2, Main Trail, drains 4.9 km². At the sampling point Stream 1 was 4.5–7.5 m and Stream 2 was 3.5–5 m wide depending on water level.

2.5. Hydrological and Water Chemistry Measurements

Water chemistry (pH, conductivity, dissolved oxygen, and temperature; Troll9500, In-Situ Inc., USA) and stage height (Rugged Troll, In-Situ Inc., USA) were continuously logged every 15 min in these streams from February 2011 to October 2012. The water chemistry is important as the continuous time series could be used to predict C concentrations, and stage height is needed to calculate export budgets. Flow velocity (Flowlink2150, ISCO Inc., USA) was monitored in either stream in turn as campaigns and stream cross sections measured periodically. As flow velocity is the key control for CO_2 outgassing [*Long et al.*, 2015] we focused on deriving a flow velocity time series from the stage to velocity relationship (Figure S2) and then calculated discharge from velocity and the active cross section at given stage height.

During the study period the stage height ranged between 24 and 717 cm and between 0 and 90 cm in Streams 1 and 2, respectively. The stage velocity regression obtained for Stream 1 would yield high-velocity estimates at high stage height values, whereas based on field observations, the stream velocity would start to decrease when stage height exceeded 100 cm and would have ceased completely by 180 cm stage height. There were a limited number of velocity measurements from flooded conditions as the flow logger unit could not be deployed during those periods due to the risk of damaging or losing the unit. A linear decrease in flow velocity was assumed between 100 cm to 180 cm stage heights.

The stage to velocity relationship in Stream 1 was complicated as the fastest-flowing section was at times diverted by debris trapped between the rocks in the river bed; thus, similar stage heights could be associated with wide range of flow velocities (Figure S2). However, an exponential increase in velocity was not considered realistic, so the linear relationship was fitted but with the high predictions during flooding adjusted based on field observations as described above. The stage to flow velocity conversion appears to overpredicting in the lower velocity range. However, this velocity range has a limited contribution to the total discharge with the flow <0.2 m/s contributing just 5% to the total discharge during the study period. Of more concern would be uncertainties in the predicted higher-velocity range. The calculated flow velocities >0.7 m/s contribute approximately 30% of the annual discharge. However, quantifying the error in that extrapolated range, or in the range when velocity measurements diverge ($>0.4 \, \mathrm{m \, s^{-1}}$), is difficult. To yield an estimate on the magnitude of the error in the velocity measurement, the percent residuals in the midrange of predicted velocity ($0.25–0.35 \, \mathrm{m \, s^{-1}}; n = 485$) were investigated (Figure S3). The median percent residual in this range was approximately 2% with the first and third quartiles at −25% and 23%, respectively. The mean of these quartiles (24%) was taken to describe the uncertainty associated with flow velocity estimate. To propagate the error to discharge, an estimated 10% error in the stream cross-section measurement was assumed. To investigate the effect of potential discharge overestimation in the velocity range where data was lacking ($>0.7 \, \mathrm{m \, s^{-1}}$), a sensitivity analysis was carried out by reducing the discharge in that range by 37.5% and recalculating the annual total discharge and the resulting C export.

In the case of Stream 2 the stage height to flow velocity relationship was better constrained (Figure S2). The median percent residual across the whole measurement range was approximately 3% with the first and third quartile at −6% and 10%. The resulting uncertainty in the flow velocity measurement was estimated to be the mean of the quartiles (8%), which was then propagated in the discharge data along with the estimated 10% uncertainty in the cross-section measurement.

The closure of water balance was investigated comparing the flux tower measurements of rainfall and evapotranspiration and the resulting calculated water availability to the observed streamflow. Stream 1 is perennially active as a result of a groundwater inputs, and hence, the total streamflow was split to event and base flow using the EcoHydRology package in R software, version 3.1.0. The BaseflowSeparation code applies a digital filter [*Lyne and Hollick*, 1979] to the streamflow data; three passes of the filter were used. The seasonal Stream 2 does not have a groundwater component, and the total discharge was compared to the catchment water availability.

2.6. Deriving Continuous Fluvial Carbon Export Time Series

In order to compare fluvial export with the EC estimates, detailed and continuous time series are necessary. Continuous measurement of fluvial export is not possible as sensors for all relevant C pools do not exist. Thus, the continuously logged hydrological and water chemistry data was explored to assess if these measurements formed strong relationships with directly measured values and so could be used to generate

semicontinuous time series (models) of [DIC], [DOC], and [POC]. This approach has worked successfully elsewhere [e.g., *Waldron et al.*, 2007; *Monteiro et al.*, 2014; *Zanchi et al.*, 2015]. From such concentration time series, using continuous discharge time series fluvial export can be calculated. Similarly, to understand the fraction of CO_2 that evades from aquatic systems, rather than from plant and soil respiration, a model for continuous CO_2 efflux time series was required.

Generalized linear models (glm) were fitted to the water chemistry and hydrological data using the R version 3.1.0 [*R Core Team*, 2014] to construct models to estimate the carbon concentration (DIC, DOC, and POC) and CO_2 efflux time series. These time series were then combined with discharge data to calculate annual carbon export. This full model was simplified by sequentially excluding the least significant explanatory variables to derive the best fit model. A glm model has a user-defined error structure and a link function that can be selected to ensure that the fitted values stay within a realistic range [*Crawley*, 2003]. The generalized linear models do not yield R^2 values, and therefore, the concordance correlation coefficients (ccc), which consider the influence of both location and scale shift in the relationship between two variables [*Lin*, 1989], were used to assess the quality of fit.

For [DIC], [DOC], and [POC], an identity link was used. For the CO_2 efflux a log link was selected to preclude negative predictions of CO_2 efflux; as this was never observed in field measurement and all pCO_2 values calculated from measured [DIC], pH and temperature data [*Rebsdorf et al.*, 1991] were above the atmospheric equilibrium (Stream 1: 2399–10,712 ppm; Stream 2: 1256–4205 ppm (details on stream pCO_2 are found in *Long et al.* [2015]). To build the CO_2 efflux model, the measurement of water flow velocity at the chamber's location was used. In Stream 1, the water flow velocity measured at chamber deployment spots ranged from 0.05 to $0.9 \, \text{m s}^{-1}$, with one extreme value of $1.58 \, \text{m s}^{-1}$ which was excluded from the modeling data set. Stream 1 also flooded, during which the flow stopped as the high water level in the Tambopata River, into which the small streams drained, backed up and blocked the stream water outflow. During flooded periods the model was not applied; instead, an efflux rate of $0.33 \, \mu\text{mol m}^{-2} \text{s}^{-1}$ ($n = 1$) measured during flooding in the field was used. The chamber measurements on a given day were carried out in multiple places in the stream and may not be coincident with the model projection as these spot measurements were over a range of velocities, whereas the flow velocity logger was deployed at a fixed point. In Stream 1, an alternative CO_2 efflux model based on flow velocity alone was derived; this was applied when dissolved oxygen and conductivity were outside the range observed during field measurements as the full model produced extreme predictions in these conditions.

To derive annual aquatic CO_2 efflux contribution in units that are comparable to the other measurements, the modeled efflux rate ($\mu\text{mol C m}^{-2} \text{s}^{-1}$; relating to water surface) was converted to Mg C yr^{-1} using the stream surface area calculated from mapped stream lengths and stream width estimates from different seasons. This total CO_2 efflux from the stream surface was then related to the catchment land area (as in *Billett et al.* [2004]).

Prior to producing the C time series from the water chemistry data, a gap in the Stream 1 pH data due to probe malfunctioning (1 July to 7 September 2011) was filled by using pooled coefficients derived from multiple fits (100) of a model based on conductivity and stage height (MICE package in R [*van Buuren and Groothuis-Oudshoorn*, 2011]). In Stream 2 water chemistry time series there were much larger data gaps in 2012 due to problems with the instruments. These were beyond the scope of reliable gap filling, and therefore, a more restricted C concentration time series was produced.

The best energy balance closure in the EC data was found when the wind came from the NE. Then, the tower was measuring gas exchange in a flux footprint containing Stream 1 catchment. Hence, data from this stream were more suitable for calculating the fluvial carbon export, and the site C balance focuses on these data. When continuous carbon time series were used to calculate monthly export and annual total for the period from October 2011 to September 2012, any missing values were filled with the monthly mean value. Results from Stream 2 were included to illustrate the differences found in two adjacent stream catchments draining the same forest area. Uncertainty in the estimates is expressed as standard deviation unless stated otherwise.

3. Results

3.1. Terrestrial Fluxes of CO_2

The EC measurements indicated a photosynthetic uptake of $27.2 \, \text{Mg C ha}^{-1} \text{yr}^{-1}$ and an estimated respiratory loss of $27.9 \, \text{Mg C ha}^{-1} \text{yr}^{-1}$ (Table 1). Uncertainties in these estimates cannot be calculated from the data

Table 1. Monthly Breakdown of the Eddy Covariance Carbon Sink Estimates and Fluvial Carbon Export at the Tambopata Study Site, Madre de Dios, Peru From October 2011 to September 2012[a]

	11 Oct	11 Nov	11 Dec	12 Jan	12 Feb	12 Mar	12 Apr	12 May	12 Jun	12 Jul	12 Aug	12 Sep	Total
Flux tower GPP estimate	-2,337	-2,211	-2,186	-2,404	-1,986	-2,328	-2,304	-2,114	-2,016	-2,373	-2,507	-2,414	-27,181 ± 6795
Ecosystem respiration	2,425	1,844	2,142	2,565	2,168	2,158	2,677	2,118	2,261	2,428	2,610	2,492	27,888 ± 6972
Flux tower NEE estimate	87.6	-366.6	-44.1	161.4	181.6	-169.9	372.8	4.4	244.9	54.6	103.3	77.6	708 ± 9736
DIC export	4.2 ± 1.5	4.4 ± 1.6	9.4 ± 3.3	10.7 ± 3.6	9.9 ± 3.5	12.5 ± 4.1	8.2 ± 2.6	12.5 ± 4.1	12.9 ± 4.4	13.1 ± 4.5	9.0 ± 3.2[b]	6.3 ± 2.3[b]	113 ± 11.8
DOC export	1.2 ± 0.7	1.5 ± 1.0	10.8 ± 7.0	21.5 ± 12.9	23.7 ± 17.1	28.8 ± 17.1	11.0 ± 6.4	7.6 ± 4.2	5.9 ± 3.1	6.5 ± 3.4	1.6 ± 2.3[b]	1.4 ± 01.0[b]	122 ± 29.8
POC export	2.2 ± 2.6	2.3 ± 2.7	7.9 ± 9.2	12.6 ± 14.8	12.6 ± 14.8	16.3 ± 19.0	9.2 ± 10.7	8.9 ± 10.4	7.8 ± 9.2	8.4 ± 9.8	4.8 ± 5.6[b]	3.3 ± 3.8[b]	96 ± 36.7
Total fluvial carbon export	7.7	8.2	28.2	44.9	46.2	57.6	28.4	28.9	26.7	28.0	15.5[b]	11.0[b]	331 ± 48.7
Total C loss from the site (NEE + fluvial)													1 039

[a]Sign convention: negative means uptake of carbon from the atmosphere. The aquatic carbon export values are based on Stream 1 that is directly draining the flux tower footprint area. The units are in kg C ha^{-1} month^{-1} for all the other columns except the total which is kg C ha^{-1} yr^{-1}. The uncertainties in the fluvial export have been derived propagating the uncertainties from the C concentration model and discharge calculation. On annual level the uncertainty related to the EC measurements was taken to be 25% according to *Kruijt et al.* [2004].
[b]These values come with a larger uncertainty as the pressure sensor data to derive stage height and discharge did not appear to record a fairly large rain event, and so its functioning may be limited.

collected here, as many of the errors on eddy covariance are systematic and not random. For the general case of tall forest in tropical conditions, the error sources have been discussed and estimated by *Kruijt et al.* [2004]: they include the errors associated with the inhomogeneity of the landscape and the lack of turbulence at night (and, consequently, the need to discard the majority of the nocturnal data). We have cautiously adopted the 25% error these authors have recommended for these especially challenging Amazon rain forest conditions. The resulting uncertainty is 6.8 Mg C ha^{-1} yr^{-1} on the photosynthetic uptake and 7.0 Mg C ha^{-1} yr^{-1} on the respiration, leading the estimated small source to the atmosphere of 0.7 Mg C ha^{-1} yr^{-1} to be associated a maximum uncertainty of 9.7 Mg C ha^{-1} yr^{-1}. With such uncertainty, the direction of the site C balance cannot be verified with confidence. On a monthly basis, 9 of the 12 months showed a small carbon loss (Table 1). There was no clear seasonal pattern in the fluxes and no simple relationship with rainfall or temperature.

3.2. Stream Chemistry and Discharge

The streams in the footprint of the flux tower had low conductivity and low pH, especially Stream 2 (Table 2). The streams responded differently to rainfall. In Stream 1, the cross-correlation coefficient was highest for rain 5 h prior to the stage height measurement, whereas in Stream 2 the highest correlation was with precipitation 15 h before, indicating that Stream 1 responds more quickly to rainfall (Figure S3).

Annual total discharge in Stream 1 was 2705 ± 703 mm (Table 3). After base flow separation the event flow (1399 ± 364 mm) was approximately within the calculated water availability (757 ± 189 mm) when considering the related uncertainties. The flow in Stream 2 (678 ± 88 mm) was in better agreement with the calculated availability. When the sensitivity analysis described above was applied to the highest flow velocities in Stream 1 data, the annual event flow was reduced to 1161 mm which is in closer agreement with the calculated availability. In terms of the annual fluvial C export this reduction in discharge would translate into 15% reduction in C loss. Uncertainty is unavoidable due to estimating discharge dur-

Table 2. Water Chemical, Hydrological, and Fluvial Carbon Values of the Streams Sampled at the Tambopata Site, Madre de Dios, Peru, February 2011 to September 2012[c]

Sampling Location	pH	Conductivity (μS cm^{-1})	Dissolved Oxygen (% Saturation)	Temperature (°C)	Stage Height (cm)[a]	Discharge (m^3 s^{-1})[a]	DIC (mg C L^{-1})	DOC (mg C L^{-1})	POC (mg C L^{-1})	CO$_2$ Efflux (μmol m^{-2} s^{-1})
Stream 1										
Mean (±SD)	6.3 (±0.3)	33 (±12)	72 (±12)	23.7 (±1.3)	58 (±66)	0.47 (±0.83)	4.5 (±2.2)	3.6 (±2.3)	5.3 (±6.8)	16.9 (±15.5)
Median	6.3	32	75	23.9	40	0.26	4.3	3.1	3.5	12.9
Range	5.0–7.1	9–76	0–90	18.8–27.5	24–717	0–5.1	1.0–9.3	0.7–12.3	1.0–54.1	0.3–79.6
n	50,784	50,784	40,265	50,765	56,610	9,053[b]	172	82	82	51
Stream 2										
Mean (±SD)	5.1 (±0.1)	7 (±2)	75 (±5)	23.9 (±1.0)	32 (±16)	0.2 (±0.2)	1.2 (±0.3)	7.0 (±1.3)	2.7 (±1.6)	4.5 (±2.5)
Median	5.1	7	75	24.0	30	0.15	1.2	6.58	2.3	4.6
Range	4.5–6.2	5–28	40–93	16.9–26.5	10–90	0.01–1.5	0.6–1.9	4.7–11.4	1.2–10.0	0.4–12.0
n	15,012	13,579	15,241	16,164	24,482	6,468[b]	104	52	53	42

[a] Stream 2 data relate to the periods that the stream was flowing.
[b] Discharge was calculated from the relationship established between stage height and flow velocity (m s^{-1}) and the detailed stream cross-section measurements.
[c] Stream 1, New Colpita, was a perennial, and Stream 2, Main Trail, was an ephemeral stream.

ing and approaching flooded conditions; estimating rainfall can be error prone too [e.g., *Mekonnen et al.*, 2015]. However, the water balance indicates that the discharge estimate was reasonable and potential errors in the higher flow range had limited impact on the total export estimates and does not change the unambiguous finding that the rivers are a net C export.

The flooding observed in Stream 1 was caused by the Tambopata River, where the streams drain, blocking the water outflow. The flooding episodes could cause backwater effects in the measurements taken at the sampling point as Tambopata water could be flowing inward and mixing with the stream water. The bulk of samples used to model DIC and DOC had been taken in nonflooded conditions, and those taken during flooding are within the range observed during nonflooded conditions (Figure S4). Hence, the models derived should not be affected by Tambopata River waters. However, since the DIC model included conductivity, and the DOC model pH and conductivity as explanatory variables, errors in the export budgets could arise due to Tambopata backwater effect on Stream 1 water chemistry from which the C concentration time series were constructed. During normal streamflow, increased stage height was accompanied with a drop in both conductivity and pH, beyond 180 cm stage height at times an increase in these variables were observed (Figure S5). This increase could be due to Tambopata water and influence the modeled carbon concentrations. However, since discharge was taken as 0 during these periods, the potential backwater effects do not influence the carbon export calculations. For POC export the median concentration was used in the calculations, and it is not subjected to issues described above for DIC and DOC.

3.3. Seasonal Patterns in Aquatic C Concentrations and Efflux

The carbon concentrations in Stream 1 varied seasonally. The mean [DIC] in Stream 1 was 4.5 ± 2.2 mg C L^{-1} and 1.2 ± 0.31 mg C L^{-1} in Stream 2, markedly lower (Table 2). The [DIC] range was wider in Stream 1 as wet and dry seasons have different groundwater contributions. During the drier season (sampled during September–December 2011), when the proportion of groundwater in the streamflow is higher, [DIC] was 6.2 ± 1.7 mg C L^{-1}, and it was significantly lower during the wet seasons (2.9 ± 1.2 mg C L^{-1}; p value < 0.0001; $n = 86$ for both wet and dry seasons). Stream 1 had lower mean [DOC] (3.6 ± 2.3 mg C L^{-1}) than Stream 2 (6.95 ± 1.3 mg C L^{-1}). In Stream 1 the wet and dry seasons had significantly different (p value < 0.01) mean [DOC]: 4.2 and 2.9 mg C L^{-1}, respectively. In Stream 1 the range in [POC] was wide, 1–54 mg C L^{-1}, with the highest concentration measured during heavy rains in the beginning of

Table 3. Flux Tower Estimated Water Availability Compared to the Discharge in the Two Study Streams

	11 Oct	11 Nov	11 Dec	12 Jan	12 Feb	12 Mar	12 Apr	12 May	12 Jun	12 Jul	12 Aug	12 Sep	Total
Rainfall (mm)	143	104	199	345	243	154	148	33	107[a]	7	32	115	1630 ± 408
Evapotranspiration (mm)	79	82	70	69	57	87	63	72	50	72	89	84	873 ± 218
Available water	64	22	129	276	186	67	85	−39	57	−65	−57	31	757 ± 189
Stream 1 total flow (mm)	63	66	224	359	348	456	260	252	219	230	135	93	2705 ± 703
Stream 1 baseflow (mm)	34	33	67	143	61	190	197	139	122	130	109	83	1306 ± 340
Stream 1 event flow (mm)	28	33	158	216	287	266	64	113	97	100	27	10	1399 ± 364
Stream 2 flow (mm)	0	0	35	146	213	159	104	21	NA	0	0	0	678 ± 88

[a]Gap filled as detailed above.

December 2011 that activated the flow of Stream 2 after the dry period. The Stream 1 maximum concentration (54 mg C L^{-1}) was more than twice as high as the next highest concentration (22.2 mg C L^{-1}). The median [POC] in Stream 1 was 3.5 ± 6.8 mg C L^{-1} and in Stream 2 2.3 ± 1.6 mg C L^{-1}. The maximum [DOC] in both streams was also observed during those heavy rains at the end of the dry season 2011, but intraevent maximum [DOC] was later than the [POC]. In Streams 1 and 2 maximum [DOC] were observed in samples collected 14 h and 21 h after the maximum [POC]. Aquatic CO_2 efflux ranged widely: 0.3–79.6 μmol m^{-2} s^{-1} in Stream 1 and 0.4–12 μmol m^{-2} s^{-1} in Stream 2. Efflux from the flooded forest was 2.4 ± 0.93 μmol m^{-2} s^{-1}.

Our POC sampling excluded the coarse fraction of carbon lost from the system which would include leaves, twigs and branches transported by the streams. However, such coarse particulate organic carbon (CPOC; collected using a sampler with a 2 mm mesh size net) has been found to be 1.5 kg C ha^{-1} yr^{1} elsewhere in the Amazon Basin [*Selva et al.*, 2007] which is only 1–1.6% of our estimated POC export. Further, in a cool-temperate deciduous system where a larger fraction of trees shed their leaves annually, the [CPOC] (total of size classes 1–10 mm and >10 mm) was 0.34 mg L^{-1} [*Shibata et al.*, 2001] which is equivalent to 10–15% of our median [POC]. Hence, it appears that the coarse particulate fraction is a minor component of the carbon export, and its omission will not lead to large underestimation of export in this study.

3.4. Models to Predict C Concentrations

The ccc values of the best fit models for the two streams ranged from 0.65 to 0.91, with the poorest value found in Stream 2 (Table 4 and Figure S6). In Stream 1, conductivity was included as an explanatory variable in all the models. Conductivity reflects the contributions of surface runoff and groundwater, with dry season characterized by higher conductivity due to proportionally greater groundwater contribution. [DOC] peaks during event flow conditions and stage height was included as explanatory variable in the model for Stream 1. No significant explanatory variables were found to predict [DOC] in Stream 2. [POC] was not successfully predicted by any model in either stream. Where a model could not be derived, the median concentrations were used to estimate export for the study year. Stream 2 had a low pH, and hence, most of the DIC pool was in form of free CO_2. The [DIC] model for this stream included dissolved oxygen saturation which is likely to be related to respiration levels in the stream. Dissolved oxygen saturation was included in the CO_2 efflux models for both streams. The efflux rate was strongly dependent on the water flow velocity, with the slope of the relationship reflecting the differences in pCO_2 (Figure S7). The model (Figures S8 and S9) shows the projected CO_2 efflux from the position that the velocity sensor was emplaced. The full CO_2 efflux model (Figure S8a) produced very high CO_2 efflux estimates when the model parameters (oxygen saturation or conductivity) were outside the range under which the model was constructed. During these conditions the efflux estimates were improved using the flow-based model (Figure S8b); however, some peak efflux rates above the measured maximum 79.6 μmol m^{-2} s^{-1} were still observed, but these had limited influence on the annual fluxes calculated.

3.5. Fluvial Carbon Time Series and Export Budgets

For the eddy covariance measurement period fairly continuous time series of the carbon species could be produced for Stream 1 (Figure 2). The number of missing values in Stream 1 each month, ranged from 0 to 496 data points (equal to 0–5 days of measurements), except for October 2011 where 15 days of data were missing. Hence, the export value for October has a greater uncertainty. Due to data gaps in the continuously logged explanatory variables, only a much shorter continuous DIC time series (Figure S10) could be derived for the ephemeral Stream 2, and therefore, the median [DIC] (Table 2) was used to calculate the annual export

Table 4. Stream Models Used to Derive the 15 min Resolution Carbon Time Series and the Concordance Correlation Coefficient for the Agreement Between Fitted and Measured Values and the Number (n) of Carbon Samples Used to Build the Model

	n	ccc	Predictive Equation
			DIC
Stream 1	172	0.91	$0.74 + 0.13 *$ conductivity
Stream 2	104	0.65	$-4.65 + 1.22 * \text{pH} + 0.014 * \text{stage height} - 0.012 * \text{dissolved oxygen}$
			DOC
Stream 1	82	0.78	$23.48 - 2.95 * \text{pH} - 0.066 * \text{conductivity} + 0.0083 * \text{stage height}$
Stream 2	52	-	No significant explanatory variables; median $6.58 \, \text{mg C L}^{-1}$ (SD 1.3)
			POC
Stream 1	82	-	No satisfactory model found; median $3.52 \, \text{mg C L}^{-1}$ (SD 4.02[a])
Stream 2	53	-	No significant explanatory variables; median $2.25 \, \text{mg C L}^{-1}$ (SD 1.6)
			CO_2 Efflux
Stream 1	46	0.87	$\text{Exp}(9.47 + 3.30 * \text{flow velocity} - 0.04 * \text{conductivity} - 0.08 * \text{dissolved oxygen})$
[b]	46	0.84	$\text{Exp}(1.92 + 3.00 * \text{flow velocity})$
Stream 2	41	0.84	$\text{Exp}(3.96 + 4.14 * \text{flow velocity} - 0.05 * \text{dissolved oxygen})$

[a]Carbon species units: DIC, DOC, POC (mg C L^{-1}), and CO_2 efflux ($\mu\text{mol m}^{-2}\text{s}^{-1}$). Explanatory variable units: Conductivity ($\mu\text{S cm}^{-1}$), pH, dissolved oxygen (% saturation), and stage height (cm). The highest value 54.1 mg C/L was excluded from this.
[b]The model based on flow velocity was used when oxygen data were missing due to probe malfunction (17 July to 4 September 2012) and when water chemistry variables were below the range observed during efflux measurements (oxygen saturation $< 64\%$; conductivity $< 19 \, \mu\text{S cm}^{-1}$).

budget. As no predictive relationship was observed for [DOC] and [POC], these export budgets (Figure S11) were also calculated using the median concentrations and discharge data (Table 2).

The wet season was far more important to mass of carbon exported (in relation to the catchment land area) by Stream 1 (Figure 3), with 71% of the annual C export taking place December to May. The effect of wet season was most pronounced for DOC with 61% of annual export taking place in January to March. [DIC] was higher during the dry season (June–November), and hence, differences in C export between dry and wet seasons are less marked, with the December–May period constituting 56% of the total DIC export. The annual total export of $331 \pm 48.7 \, \text{kg C ha}^{-1}\text{yr}^{-1}$ in Stream 1 (Table 1) consisted of 34% ($113 \pm 12 \, \text{kg C ha}^{-1}\text{yr}^{-1}$) DIC, 37% ($122 \pm 30 \, \text{kg C ha}^{-1}\text{yr}^{-1}$) DOC, and 29% ($96 \pm 37 \, \text{kg C ha}^{-1}\text{yr}^{-1}$) POC. Naturally, in the seasonal Stream 2 all the C export took place during the wet season (Figure S11). The amount exported, $66 \pm 3.5 \, \text{kg C ha}^{-1}$, was also much less than for Stream 1 ($234 \pm 45 \, \text{kg C ha}^{-1}$) for the corresponding December–May period.

Corrections for the input of C from rain and export of aged carbon are required to avoid erroneously incorporating ecosystem C loss from sources that are external or not derived from recently fixed C. The volume-weighted carbon concentrations in rain water were found to be $0.16 \pm 0.06 \, \text{mg C L}^{-1}$ of DIC ($n = 5$), $2.3 \pm 0.23 \, \text{mg C L}^{-1}$ of DOC ($n = 7$), and $1.3 \pm 0.22 \, \text{mg C L}^{-1}$ of POC ($n = 7$). During the year of comparison the rainfall was 1630 mm which would yield total deposition of approximately 0.06 ± 0.005 metric ton $\text{C ha}^{-1}\text{yr}^{-1}$.

3.6. Fluvial Carbon Export in Relation to Terrestrial CO_2 Flux

In comparison to the indicated small net source of $0.7 \, \text{Mg C ha}^{-1}\text{yr}^{-1}$ (EC) or sink $0.5 \, \text{Mg C ha}^{-1}\text{yr}^{-1}$ (a measurement from a nearby biomass plot [*Malhi et al.*, 2014]) the fluvial export is equivalent to 43–60% of these small net C fluxes. The CO_2 effluxed from drainage was a minor component, approximately 0.3–0.7%, of the plant and soil respiration (Figure 4b). The site C loss in drainage $0.3 \, \text{Mg C ha}^{-1}\text{yr}^{-1}$ was small compared to the uncertainty of the terrestrial C balance: 3% in relation to EC measurement and 7% to biomass plot study results. The fraction derived from fossil carbonate sources (estimated from *Vihermaa et al.* [2014]) is likely to be less than 1% of the fluvial export but could be a maximum of 7% (Figure 4a). Rainfall contributions were equal to approximately 20% of the fluvial export.

4. Discussion

4.1. CO_2 Fluxes: Comparisons of This Site With Other Sites in the Amazon Basin

The present eddy covariance result suggests that the forest is neither a strong source nor a strong sink but is close to being in equilibrium showing a carbon gain of $+0.7 \, \text{Mg ha}^{-1}\text{yr}^{-1}$ which corresponds to ~1% of the
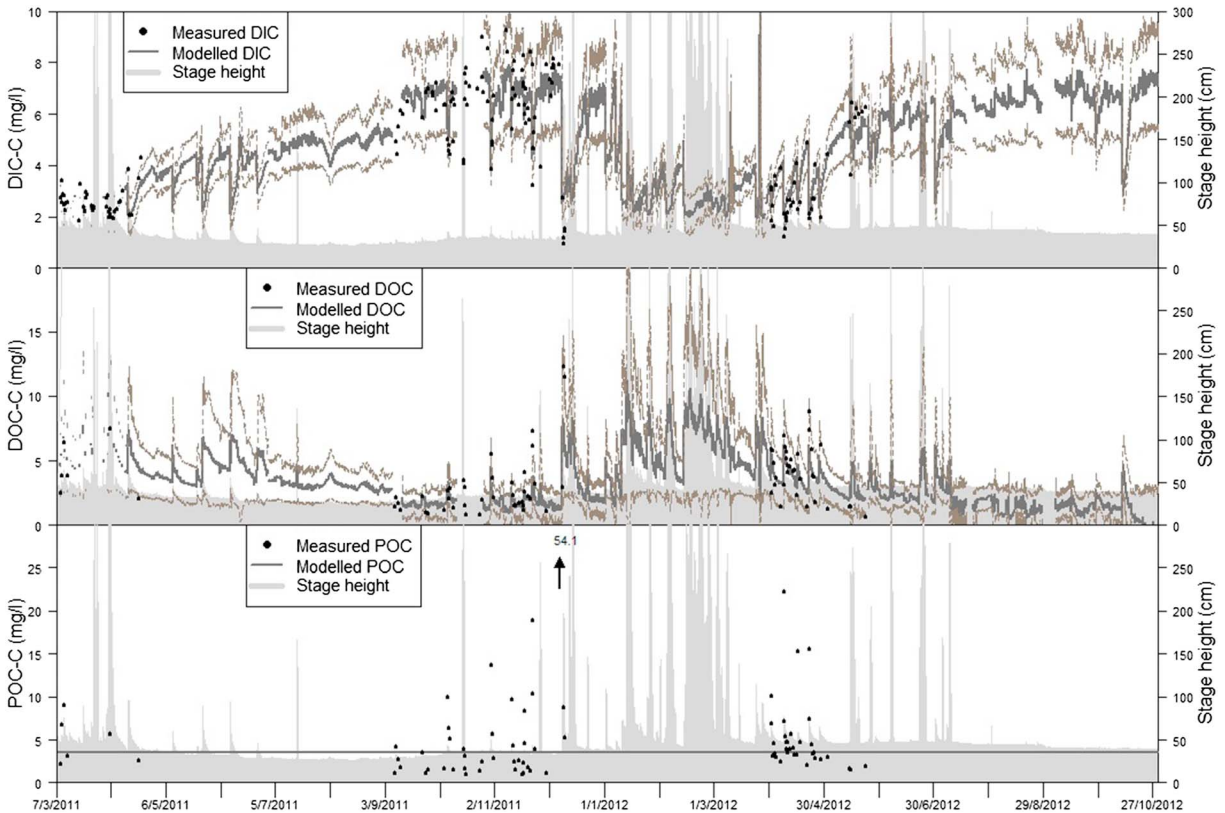
Figure 2. Full time series plots for the perennial Stream 1 that drains the tower footprint. The dashed bands around the C time series show the model uncertainty (as the standard deviation). Stage height scale maximum was set to 300 cm to keep smaller events more visible. This excludes the highest flood peaks extending to maximum of 717 cm. As no satisfactory model was found for POC the median value shown with the horizontal grey line was used to derive the annual export budget. On the graph [POC] was scaled from 0 to 25 mg L^{-1} to make the majority of values more visible, the location of maximum [POC] of 54.1 mg L^{-1} is indicated by the arrow.
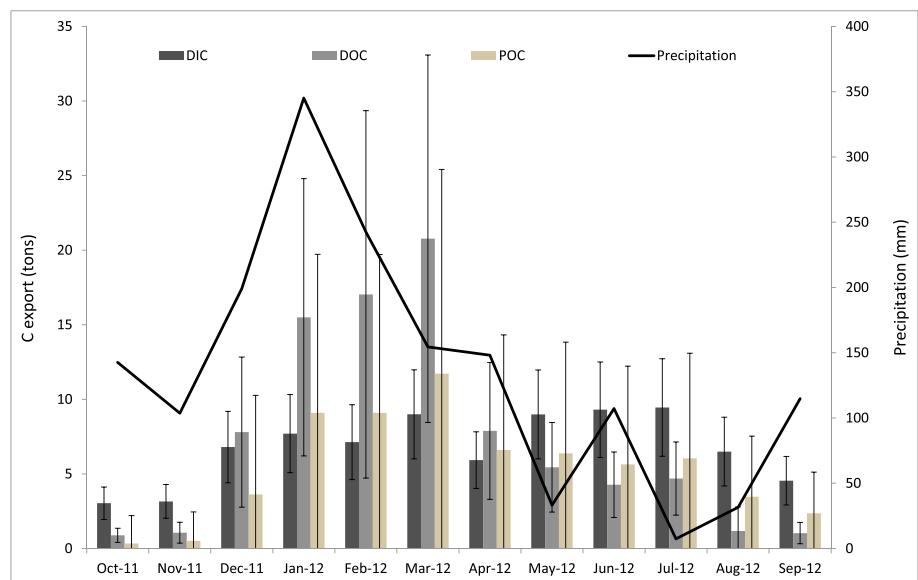
Figure 3. Monthly fluvial export (Mg C) as DIC, DOC, POC, and precipitation. Values are calculated from the Stream 1 time series (Figure 2) as this stream drains the tower footprint more directly. The uncertainties in the monthly export values have been calculated by propagating the errors in the concentration model predictions and discharge measurements.
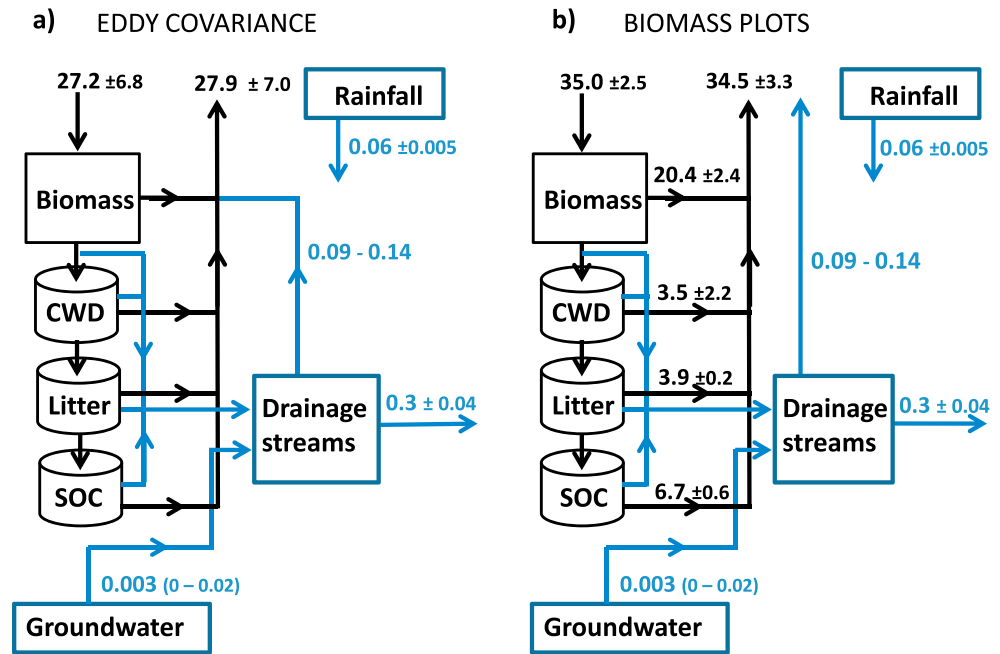
Figure 4. Carbon balance of the Tambopata site with the aquatic fluxes (blue) related to terrestrial fluxes (black) from (a) eddy covariance results of this study and (b) biomass plot data. The range in aquatic CO_2 efflux spans the estimates derived using the full model, flow only model and simply the median efflux rate. The fluvial C export is calculated using the modeled [POC] results and those based on the median [POC]. The biomass plot terrestrial fluxes are from *Malhi et al.* [2014], with coarse woody debris (CWD) contribution from *Gurdak et al.* [2014] and litter respiration estimates as a balance from inputs (Y. Malhi, personal communication, 2014). SOC stands for soil organic carbon and CWD for coarse woody debris. All units are $Mg\,C\,ha^{-1}\,yr^{-1}$; the aquatic values have been converted to relate to catchment land area.

standing biomass of the forest surrounding the tower. Biomass plot observations incorporating multiple years have also indicated the study site to have a close to neutral C balance [*Malhi et al.*, 2014]. There have been no previous eddy covariance flux measurements in the Peruvian Amazon, which represents the extreme west of the Amazon Basin and contains soils which are significantly more base rich than those in the Brazilian Amazon [*Quesada et al.*, 2010]. The forests in the West differ from other parts of the Amazonian basin, also in terms of forest functioning, with the western forests being characterized by lower height [*Feldpausch et al.*, 2011] and faster turnover rate [*Johnson et al.*, 2016].

Measurements with this technique made at five sites elsewhere in the Amazon Basin suggest the forests to be a carbon sink [*Kruijt et al.*, 2004; *Restrepo-Coupe et al.*, 2013]. In forest within a black water catchment area, the C sink was $3–4\,Mg\,C\,ha^{-1}\,yr^{-1}$ [*Waterloo et al.*, 2006]. The mean C sink of tropical forest has been estimated as $4.0 \pm 1.0\,Mg\,C\,ha^{-1}\,yr^{-1}$ [*Luyssaert et al.*, 2007], although this is based on only a few sites and may not be a representative. An average annual loss of $1.3\,Mg\,C\,ha^{-1}\,yr^{-1}$ over the 3 year study period was detected in a rainforest near Santarém, Brazil [*Saleska et al.*, 2003]. In the western part of the Amazon Basin in Brazilian state of Rondônia interannual variations between source and sink were measured over the period from 2004 to 2010 as a response to available moisture in the previous year. On average, that Rondônian site was a C sink of approximately $5\,t\,C\,ha^{-1}\,yr^{-1}$ but with interannual variation from a source of $1.2 \pm 2.1\,Mg\,C\,ha^{-1}$ to a sink of $10.4 \pm 1.2\,1\,Mg\,C\,ha^{-1}$ [*Zeri et al.*, 2014]. Moreover, aircraft-based measurements show that the Amazonian landscape at a large scale, in the absence of fire, is a sink of about $0.25 \pm 0.14\,Pg\,C\,yr^{-1}$ during wet years but carbon neutral during dry years as drought suppresses photosynthesis [*Gatti et al.*, 2014]. During wet seasons, recalculated on a hectare basis, the *Gatti et al.* [2014] results would yield a small source of $0.07\,Mg\,C\,ha^{-1}\,yr^{-1}$ during the 2010 drought year and a sink of $0.65\,Mg\,C\,ha^{-1}\,yr^{-1}$ in 2011. Clearly, there can be significant inter-annual variation, and the forest C sink is sensitive to moisture conditions.

During the observation year, rainfall at our study site (1630 mm) was considerably lower than the long-term average (2377 mm). Further evidence that 2011–2012 was a dry year comes from hydrological data collected within the SO HyBAM (Geodynamical, hydrological and biogeochemical control of erosion/alteration and

material transport in the Amazon, Orinoco and Congo basins) observatory network [*HyBAM observatory network*, 2014] downstream on the Madeira River at Porto Velho. This sampling point is influenced by Madre de Dios and Bolivian tributaries (Beni and Mamoré) and hence records regional rather than local water balance. It has 45 years of measured water levels compared to only 6 years of satellite-based level observations close to Puerto Maldonado. The minimum annual dry season water level at Porto Velho in 2010 was 292 cm, in 2011 was 322 cm, and in 2012 was 315 cm, all below the 45 year median of 355 cm. These low dry season water levels indicate that the forests in this region might be suffering from a drought inheritance effect [*Phillips et al.*, 2010] which would likely decrease the carbon sink. Hence, the current EC sink estimate is likely to be below the historical long-term average.

4.2. Comparison of Aquatic C Concentrations and Fluxes With Other Sites

Similar to elsewhere in the Amazon Basin our study streams have relatively low pH and electrical conductivity [*Johnson et al.*, 2006; *Monteiro et al.*, 2014; *Neu et al.*, 2011; *Sousa et al.*, 2008; *Waterloo et al.*, 2006]. The range of [DIC], 0.6–9.3 mg C L^{-1}, observed at our site was similar to previous studies within the basin. Across the national border, in the Brazilian state of Acre, [DIC] ranged from 1.0 to 7.8 mg C L^{-1} [*Salimon et al.*, 2013; *Sousa et al.*, 2008]. In a study covering a range of Amazonian stream/river sizes and types, [DIC] ranged from 1.25 to 105 mg C L^{-1} [*Ellis et al.*, 2012]. The range of [DOC] observed here (0.7–12.3 mg C L^{-1}) was within the range observed elsewhere in the Amazon Basin, 0.3–31.3 mg C L^{-1} [*Ellis et al.*, 2012; *Johnson et al.*, 2006; *Neu et al.*, 2011; *Saunders et al.*, 2006; *Waterloo et al.*, 2006]. The [POC] maximum (54 mg C L^{-1}) was above the range 0.5–9 mg C L^{-1} observed in most studies within the basin [*Aufdenkampe et al.*, 2007; *Neu et al.*, 2011; *Waterloo et al.*, 2006]. The POC concentrations and export from the Tanguro Ranch site were very low, attributed to the almost complete lack of storm flow at this site in the savanna rainforest transition zone [*Neu et al.*, 2011]. In the Pachitea basin in the Ucuyali headwaters [POC] was low, 0.1–0.4 mg C L^{-1}, during dry season [*Townsend-Small et al.*, 2007], but in storm flows the maximum values reached 24–52 mg C L^{-1} [*Townsend-Small et al.*, 2008] which is similar to that observed at our site.

The assumption that 50% of weight loss during LOI is C may also cause some uncertainty in the POC results particularly in the case of samples collected during event flow when highest [POC] were detected. In other tropical rivers it has been found that the LOI C content is considerably lower (e.g., in Taiwan [*Hilton et al.*, 2010]). Only one study has addressed the C content of Amazonian headwater stream POM [*de Paula et al.*, 2016]. Using Walkley-Black titrations, they defined fine POM (0.45 μm–1 mm) and coarse POM (>1 mm) to contain 14–25% and 25–42% of C, respectively. However, while LOI has been found to overestimate, Walkley-Black method was underestimating C content when compared to elemental analysis [*Fernandes et al.*, 2015]. Regardless of the uncertainty on the most appropriate C content value to be applied, our POC export is robust and conservative as we based it on the median [POC], excluding these high range values prone to overestimation.

Previously measured Amazon rainfall [DOC] ranges from 0.3 to 4.4 mg C L^{-1} [*Andreae et al.*, 1990; *Ciglasch et al.*, 2004; *McDowell*, 1998; *Waterloo et al.*, 2006] which encompasses the value observed here (2.3 ± 0.23 mg C L^{-1}).

Floating chamber measurements of CO$_2$ fluxes yielded mean effluxes of 16.8 (±15.5) μmol C m^{-2} s^{-1} and 4.5 (±2.5) μmol C m^{-2} s^{-1} from Streams 1 and 2, respectively. The mean from Stream 1 is close to the mean efflux from a Brazilian headwater stream, 16 μmol C m^{-2} s^{-1} [*Neu et al.*, 2011]. In third- to fourth-order streams in the Ji-Paraná basin emissions ranged from 0.67 to 12.63 μmol C m^{-2} s^{-1} [*Rasera et al.*, 2008]. CO$_2$ efflux from Stream 1 contains old carbon which most likely originates from carbonate weathering and is delivered in groundwater [*Vihermaa et al.*, 2014]. Such carbon fractions constitute a nonecosystem-derived component, and so a correction of 0.003 Mg ha^{-1} yr^{-1} is applied to the estimates of C efflux for comparison with the eddy covariance budgets. No relationship was found between [DOC], and the age of CO$_2$ evasion and Stream 2 with highest [DOC] had the youngest age, indicating that DOC was unlikely to contain old carbon [*Vihermaa et al.*, 2014]. Further, the results suggested that in situ decomposition of POC was not the source of aged CO$_2$ efflux [*Vihermaa et al.*, 2014]. This does not preclude old POC being transported in these streams, but this material is likely to be restricted to soil or black carbon-derived fractions which still originate from the local ecosystems [*Vihermaa et al.*, 2014], as fossil POC is typically derived from shale weathering in mountainous areas [*Clark et al.*, 2013, *Copard et al.*, 2007].

The annual total discharge (2705 ± 703 mm) was higher than the estimated available water (757 ± 189 mm). This is closer to event flow (1399 ± 364 mm), and although the uncertainties in the estimates bring these

values closer together, other water may be entering into the catchment, e.g., groundwater or within terrace storage. Groundwater delivered from outside the catchment area may lead to over estimation of fluvial C export if also delivering dissolved C. However, [DOC] is low in groundwater prior to contact with the riparian zone [*Johnson et al.*, 2006], and hence, this effect would be limited to DIC which accounted for third of the fluvial C loss. High CO_2 concentration delivered in groundwater is quickly lost with 90% degassed just 50 m downstream from a spring [*Johnson et al.*, 2008]; hence, at our sampling point groundwater-derived DIC should largely have been lost. Data collected from downstream of groundwater spring elsewhere at our site showed DIC concentrations (11 mg L^{-1}; $n = 10$); even though already subjected to degassing, it is well above the mean dry season concentration (6.2 mg L^{-1}) found in Stream 1. Emerging groundwater had been measured to contain 21.1 mg CO_2 C L^{-1} ($n = 47$ [*Johnson et al.*, 2008]). Using this value, Stream 1 [DIC] and Stream 2 [DIC] as the signature not influenced by groundwater in a simple mixing model indicate that the fraction of DIC exported potentially affected is 25%.

Our annual DOC (122 ± 30 kg C ha^{-1} yr^{-1}) and DIC (113 ± 12 kg C ha^{-1} yr^{-1}) exports from Stream 1 were within the range of the previous studies, but POC (96 ± 37 kg C ha^{-1} yr^{-1}) was considerably higher. From other sites within the Amazon Basin, annual export of DOC, DIC, and POC have been found to be, respectively, 6.4 to 470 kg C ha^{-1} yr^{-1} [*Johnson et al.*, 2006; ; *Waterloo et al.*, 2006; *Neu et al.*, 2011; *Salimon et al.*, 2013; *Monteiro et al.*, 2014; *Zanchi et al.*, 2015], 9.7 to 116 kg C ha^{-1} yr^{-1} [*Neu et al.*, 2011; *Salimon et al.*, 2013], and 0.01 to 17.8 kg C ha^{-1} yr^{-1} [*Johnson et al.*, 2006; *Neu et al.*, 2011; *Waterloo et al.*, 2006]. Fossil C transported by Stream 1 is likely to be <10%, most likely within the DIC pool possibly with some contribution from the POC pool, whereas DOC export is unlikely to contain highly aged fractions [*Vihermaa et al.*, 2014]. While further research is required to better constrain the origins of fossil/aged C in this area, it can be concluded that the main bulk of the material is likely to be recently fixed C.

This research assesses the importance of fluvial C export as permanent loss of ecosystem C from the site (=the EC flux footprint) to understand better the site C balance. However, when exported further downstream within the Amazonian basin, these C pools will undergo various cycles of processing (decomposition, degassing, photosynthetic uptake, deposition of floodplains, burial, and resuspension). Thus, at the scale of the wider Amazonian ecosystem the C released from the study site may be reutilized several times. For example, any recently fixed POC delivered to the mouth of the Amazon could contribute to the ocean C sink, although this delivery from the Western Amazon will be less important than in small mountain rivers where the transit times to the ocean are much shorter [e.g., *Hilton et al.*, 2010].

4.3. Influence of Fluvial Carbon Export on the Site C Balance

In a black water Amazonian catchment organic carbon export alone (DOC + POC; 92–94% of carbon in dissolved form) averaged 190 kg C ha^{-1} yr^{-1} and when included in a site balance decreased the eddy covariance estimated sink strength of 3–4 Mg C ha^{-1} yr^{-1} by 5–6% [*Waterloo et al.*, 2006]. In another study, the same Asu catchment was found to lose 2.5–5% of the C sink as DOC export [*Monteiro et al.*, 2014]. Based on limited measurements of degassing in the same area, it was estimated that this site was losing >15% of NEE in lateral transport as CO_2 and inorganic carbon [*Aufdenkampe et al.*, 2011], and at this site, fluvial C export could remove as much as 20% of NEE. Amazonian heath forests have particularly high-DOC export (470 kg C ha^{-1} yr^{-1}) [*Zanchi et al.*, 2015] and hence may lose an even larger fraction of the C fixed in drainage.

The CO_2 efflux to the atmosphere from Stream 1 (per catchment land area) was estimated as 0.09–0.14 Mg C ha^{-1} yr^{-1}, which appears as a minor component in comparison to terrestrial respiration fluxes at the Tambopata site (Figure 4). Although the CO_2 efflux rate from Stream 1 was approximately four times of that measured for soil respiration (3 μmol m^{-2} s^{-1}; calculated as average of TAM5 and TAM6 biomass plots [*Malhi et al.*, 2014]), the contribution remained small due to limited area covered by the stream surface. During the wet season, a large part of the forest is flooded with accumulated rainwater, and hence, the surface area for aquatic CO_2 efflux greatly increases. However, the average efflux from the flooded forest (2.4 ± 0.93 μmol m^{-2} s^{-1}) then was comparable to soil respiration.

During the study year the fluvial export from our site was 0.3 ± 0.04 Mg C ha^{-1} yr^{-1}. However, there is likely to be significant interannual variability in the fluvial export fluxes. In boreal ecosystems the fluvial export has been found to be closely linked to precipitation with wetter years resulting into greater C export and reduced

photosynthetic C fixation [*Öquist et al.*, 2014]. Such long-term assessments are not yet available for the Amazonian Basin. However, with limited fluctuations in light availability and temperature during the year at Tambopata, the monthly C export data (Figure 3) can be used to assess the effect of discharge on the C export. During the wettest months, January–March, the DOC and POC exports were highest, but [DIC] is diluted during event flows, and the highest export takes place during drier months, with less pronounced intraannual variability than the organic fractions. Hence, during wetter years it is anticipated that the organic export would increase but the inorganic C export will decrease. In the Amazonian rainforest, drought periods have been found to suppress the forest growth [*Gatti et al.*, 2014] and increase mortality [*Phillips et al.*, 2010]; therefore, the double effect of precipitation (increasing fluvial export and decreasing ecosystem C uptake) observed in boreal ecosystems [*Öquist et al.*, 2014] should not take place. Instead, forest growth and fluvial C export are more likely to vary together, leading lesser interannual differences in site C balance than were observed in boreal forests. However, it is forecast that in the Amazon Basin, the wet seasons will get wetter and dry season drier [*Gloor et al.*, 2013] which may cause the ecosystems multiple stresses and hence has potential to cause more complex patterns in both terrestrial and fluvial systems. A further challenge to the construction of an annual site C balance is that some processes (such as POC erosion, DIC weathering, and persistence of drought suppression) operate on longer time scales. Therefore, long-term studies are required to yield a more refined estimate of the site C balance and quantify the fluctuations with climate.

Depending on the terrestrial C sink estimates (e.g., section 4.1), aquatic fluxes may constitute a significant loss of carbon. However, results may not be transferable as adjacent streams can be quite different (compare Streams 1 and 2), and therefore, it is important to construct an integrated carbon balance at site level. Tropical sites vary from a source of $1.3 \, t \, C \, ha^{-1} \, yr^{-1}$ to a sink of a maximum of $10.4 \, Mg \, C \, ha^{-1} \, yr^{-1}$. Within this range the fluvial export measured at our site would always constitute a significant contribution, ranging from a 23% increase of C loss at the minimum forest sink estimate to 3% reduction in the sink strength at the maximum estimate. At our study site, the fluvial export increases the C loss by 43%. The CO_2 efflux from Stream 1 alone would range in significance from 7 to 11% fraction of the total efflux to atmosphere to a flux to the atmosphere corresponding to approximately 1% of the maximum site sink.

Downstream processing of the exported C pools has important implications on the significance of these fractions for climate change. The DOC pool is likely to be decomposed relatively rapidly [*Galy et al.*, 2015; *Mayorga et al.*, 2005] and hence transfer into DIC pool and contribute to the degassing of CO_2. If POC escapes decomposition (as discussed in more detail in, e.g., *Bouchez et al.* [2010] and *Galy et al.* [2015]) and is delivered to the ocean sink, it will constitute a removal of C from atmosphere due to being recently fixed.

5. Conclusions

The eddy covariance measurements indicated that the site was close to carbon equilibrium ($+0.7 \, Mg \, C \, ha^{-1} \, yr^{-1}$) during the study year (October 2011 to September 2012). This close to neutral C balance is consistent with findings from longer-term biomass plot observations at a nearby site [*Malhi et al.*, 2014]. However, the fluvial export was unambiguously a loss from the site, and during the study year it was $0.3 \pm 0.04 \, Mg \, C \, ha^{-1} \, yr^{-1}$.

The quantification of a site C balance is clearly challenging with difficulties arising from applying EC to tropical conditions (with much missing data at night due to low $u*$ and other difficulties [*Kruijt et al.*, 2004]) and, in the biomass plot approach, the statistical uncertainty from the scaled-up data. Further, there is large interannual variability that may arise as a result of differences in precipitation with drought effects persisting several years [*Saatchi et al.*, 2013; *Zeri et al.*, 2014]. Biomass plot data that incorporated measurements over a 5 year period suggested the site to be a small sink of $0.5 \, Mg \, C \, ha^{-1} \, yr^{-1}$ (range of uncertainty spanned from a source of 3.7 to a sink of $4.6 \, t \, C \, ha^{-1} \, yr^{-1}$) [*Malhi et al.*, 2014] which is of comparable magnitude with our EC measurements. Given the uncertainty involved in all of the methods of site C balance determination, an integrated approach combining EC, biomass plots, and aqueous sampling should be adopted. Ideally, longer-term assessment would be carried out to better address the climatic variability and its effects on the C balance which would manifest themselves at different time scales depending on the measurement method. The quantification and reduction of the errors involved in EC measurements should also be addressed in future studies. Also, a more detailed hydrological assessment (including sampling of groundwater flows) should be carried out and longer-term water balance assessed.

Fluvial C export will be of crucial importance, especially at sites with close to neutral C balance, and does need to be considered in any site C balance—globally, not just the Amazon. Otherwise, we may well overestimate the sink strength and risk missing changes in the system behavior. CO_2 effluxed from aquatic systems within a flux tower footprint is accounted for when assessing the forest sink strength from the eddy covariance data, but it is still important to quantify and separate it from the soil and plant respiration as these pathways of carbon movement may differ in their response to climate change. Hence, to understand ecosystem functioning in detail, the relative magnitude of different pathways needs to be known. Further, changes in the rate of C loss in drainage could be an important indicator of disturbance or climate change impact. For example, forecasted higher-intensity rain [Gloor et al., 2013] could mobilize higher-POC concentrations and lead to an increase in C loss from a site, but this would not be evident in site balances calculated from either biomass plot data or eddy covariance, unless the export increased fluvial CO_2 efflux within the footprint of the tower. Detecting such sensitive processes is a key global challenge for the future.

References

Achard, F., H. D. Eva, H. J. Stibig, P. Mayaux, J. Gallego, T. Richards, and J. P. Malingreau (2002), Determination of deforestation rates of the world's humid tropical forests, *Science*, 297(5583), 999–1002.

Andreae, M. O., R. W. Talbot, H. Berresheim, and K. M. Beecher (1990), Precipitation chemistry in central Amazonia, *J. Geophys. Res.*, 95, 16,987–16,999, doi:10.1029/JD095iD10p16987.

Araujo, A. C., et al. (2002), Comparative measurements of carbon dioxide fluxes from two nearby towers in a central Amazonian rainforest: The Manaus LBA site, *J. Geophys. Res.*, 107(D20), 8090, doi:10.1029/2001JD000676.

Atjay, G. L., P. Ketner, and P. Duvigneaud (1977), Terrestrial primary production and phytomass, in *The Global Carbon Cycle*, edited by B. E. Bolin et al., pp. 129–181, John Wiley, New York.

Aubrecht, D. M., B. R. Helliker, M. L. Goulden, D. A. Robertsd, C. J. Stille, and A. D. Richardson (2016), Continuous, long-term, high-frequency thermal imaging of vegetation: Uncertainties and recommended best practices, *Agric. For. Meteorol.*, 228, 315–326.

Aufdenkampe, A. K., E. Mayorga, J. I. Hedges, C. Llerena, P. D. Quay, J. Gudeman, A. V. Krusche, and J. E. Richey (2007), Organic matter in the Peruvian headwaters of the Amazon: Compositional evolution from the Andes to the lowland Amazon mainstem, *Org. Geochem.*, 38(3), 337–364.

Aufdenkampe, A. K., E. Mayorga, P. A. Raymond, J. M. Melack, S. C. Doney, S. R. Alin, R. E. Aalto, and K. Yoo (2011), Riverine coupling of biogeochemical cycles between land, oceans, and atmosphere, *Front. Ecol. Environ.*, 9(1), 53–60.

Bartlett, K. B., P. M. Crill, J. A. Bonassi, J. E. Richey, and R. C. Harriss (1990), Methane flux from the Amazon river floodplain—Emissions during rising water, *J. Geophys. Res.*, 95, 16,773–16,788, doi:10.1029/JD095iD10p16773.

Billett, M. F., S. M. Palmer, D. Hope, C. Deacon, R. Storeton-West, K. J. Hargreaves, C. Flechard, and D. Fowler (2004), Linking land-atmosphere-stream carbon fluxes in a lowland peatland system, *Global Biogeochem. Cycles*, 18, GB1024, doi:10.1029/2003GB002058.

Bouchez, J., O. Beyssac, V. Galy, J. Gaillardet, C. France-Lanord, L. Maurice, and P. Moreira-Turcq (2010), Oxidation of petrogenic organic carbon in the Amazon floodplain as a source of atmospheric CO_2, *Geology*, 38, 255–258.

Boyd, D. S., R. A. Hill, C. Hopkinson, and T. R. Baker (2013), Landscape-scale forest disturbance regimes in southern Peruvian Amazonia, *Ecol. Appl.*, 23(7), 1588–1602.

Carswell, F. E., et al. (2002), Seasonality in CO_2 and H_2O flux at an eastern Amazonian rain forest, *J. Geophys. Res.*, 107(D20), 8076, doi:10.1029/2000JD000284.

Chou, W. W., C. S. Wofsy, R. C. Harriss, J. C. Lin, C. W. Gerbig, and G. W. Sachse (2002), Net fluxes of CO_2 in Amazonia derived from aircraft observations, *J. Geophys. Res.*, 107(D22), 4614, doi:10.1029/2001JD001295.

Ciglasch, H., J. Lilienfein, K. Kaiser, and W. Wilcke (2004), Dissolved organic matter under native Cerrado and *Pinus caribaea* plantations in the Brazilian savanna, *Biogeochemistry*, 67(2), 157–182.

Clark, K. E., Y. Malhi, M. New, R. G. Hilton, A. J. West, D. R. Groecke, C. L. Bryant, P. L. Ascough, and A. Robles Caceres (2013), New views on "old" carbon in the Amazon River: Insight from the source of organic carbon eroded from the Peruvian Andes, *Geochem. Geophys. Geosyst.*, 14, 1644–1659, doi:10.1002/ggge.20122.

Copard, Y., P. Amiotte-Suchet, and C. Di-Giovanni (2007), Storage and release of fossil organic carbon related to weathering of sedimentary rocks, *Earth Planet. Sci. Lett.*, 258, 345–357.

Costa, M. H., and J. A. Foley (2000), Combined effects of deforestation and doubled atmospheric CO_2 concentrations on the climate of Amazonia, *J. Clim.*, 13(1), 18–34.

Crawley, M. J. (2003), *Statistical Computing—An Introduction to Data Analysis Using S-Plus*, John Wiley, Chichester, U. K.

de Paula, J. D., F. J. Luizão, and M. T. F. Piedade (2016), The size distribution of organic carbon in headwater streams in the Amazon Basin, *Environ. Sci. Pollut. Res.*, 23, 11,461–11,470.

Devol, A. H., P. D. Quay, J. E. Richey, and L. A. Martinelli (1987), The role of gas exchange in the inorganic carbon, oxygen and Rn-222 budgets of the Amazon river, *Limnol. Oceanogr.*, 32(1), 235–248.

Ellis, E. E., J. E. Richey, A. K. Aufdenkampe, A. V. Krusche, P. D. Quay, C. Salimon, and H. B. da Cunha (2012), Factors controlling water-column respiration in rivers of the central and southwestern Amazon Basin, *Limnol. Oceanogr.*, 57(2), 527–540.

Feldpausch, T. R., et al. (2011), Height-diameter allometry of tropical forest trees, *Biogeosciences*, 8, 1081–1106.

Fernandes, R. B. A., I. A. de Carvalho Jr., E. S. Ribeiro Jr., and E. S. Mendonça (2015), Comparison of different methods for the determination of total organic carbon and humic substances in Brazilian soils, *Rev. Ceres*, 62(5), 496–501.

Frankignoulle, M. (1988), Field measurements of air sea CO_2 exchange, *Limnol. Oceanogr.*, 33(3), 313–322.

Galy, V., B. Peucker-Ehrenbrink, and T. Eglinton (2015), Global carbon export from the terrestrial biosphere controlled by erosion, *Nature*, 521, 204–208.

Gatti, L. V., J. B. Miller, M. T. S. D'Amelio, A. Martinewski, L. S. Basso, M. E. Gloor, S. Wofsy, and P. Tans (2010), Vertical profiles of CO_2 above eastern Amazonia suggest a net carbon flux to the atmosphere and balanced biosphere between 2000 and 2009, *Tellus, Ser. B*, 62(5), 581–594.

Gatti, L. V., et al. (2014), Drought sensitivity of Amazonian carbon balance revealed by atmospheric measurements, *Nature*, *506*(7486), 76–80.

Gibbs, H. K., S. Brown, J. O. Niles, and J. A. Foley (2007), Monitoring and estimating tropical forest carbon stocks: Making REDD a reality, *Environ. Res. Lett.*, *2*(4), 045023.

Gilmanov, T. G., et al. (2007), Partitioning European grassland net ecosystem CO_2 exchange into gross primary productivity and ecosystem respiration using light response function analysis, *Agric. Ecosyst. Environ.*, *121*(1-2), 93–120.

Gloor, E., et al. (2012), The carbon balance of South America: A review of the status, decadal trends and main determinants, *Biogeosciences*, *9*(12), 5407–5430.

Gloor, E., R. Brienen, D. Galbraith, T. R. Feldpausch, J. Schöngart, J.-L. Guyot, J. C. Espinoza, J. Lloyd, and O. L. Phillips (2013), Intensification of the Amazon hydrological cycle over the last two decades, *Geophys. Res. Lett.*, *40*, 1729–1733, doi:10.1002/grl.50377.

Grace, J., E. Mitchard, and E. Gloor (2014), Perturbations in the carbon budget of the tropics, *Global Change Biol.*, *20*(10), 3238–3255.

Gulliver, P., S. Waldron, E. M. Scott, and C. L. Bryant (2010), The effect of storage on the radiocarbon, stable carbon and nitrogen isotopic signatures and concentrations of riverine DOM, *Radiocarbon*, *52*(3), 1113–1122.

Gurdak, D. J., et al. (2014), Assessing above-ground woody debris dynamics along a gradient of elevation in Amazonian cloud forests in Peru: Balancing above-ground inputs and respiration outputs, *Plant Ecol. Diversity*, *7*(1-2), 143–160.

Hill, R. A., D. S. Boyd, and C. Hopkinson (2011), Relationship between canopy height and Landsat ETM plus response in lowland Amazonian rainforest, *Remote Sens. Lett.*, *2*(3), 203–212.

Hilton, R. G. (2016), Climate regulates the erosional carbon export from the terrestrial biosphere, *Geomorphology*, doi:10.1016/j.geomorph.2016.03.028.

Hilton, R. G., A. Galy, N. Hovius, M.-J. Horng, and H. Chen (2010), The isotopic composition of particulate organic carbon in mountain rivers of Taiwan, *Geochim. Cosmochim. Acta*, *74*, 3164–3181.

HyBAM observatory network (2014), [Available at http://www.ore-hybam.org.]

Johnson, M. O., et al. (2016), Variation in stem mortality rates determines patterns of aboveground biomass in Amazonian forests: Implications for dynamic global vegetation models, *Global Change Biol.*, doi:10.1111/gcb.13315.

Johnson, M. S., J. Lehmann, E. C. Selva, M. Abdo, S. Riha, and E. G. Couto (2006), Organic carbon fluxes within and streamwater exports from headwater catchments in the southern Amazon, *Hydrol. Processes*, *20*(12), 2599–2614.

Johnson, M. S., J. Lehmann, S. Riha, A. V. Krusche, J. E. Richey, J. P. H. B. Ometto, and E. G. Couto (2008), CO_2 efflux from Amazonian headwater streams represents a significant fate for deep soil respiration, *Geophys. Res. Lett.*, *35*, L17401, doi:10.1029/2008GL034619.

Kruijt, B., J. A. Elbers, C. von Randow, A. C. Araujo, P. J. Oliveira, A. Culf, A. O. Manzi, A. D. Nobre, P. Kabat, and E. J. Moors (2004), The robustness of eddy correlation fluxes for Amazon rain forest conditions, *Ecol. Appl.*, *14*(4), S101–S113.

Lean, J., and D. A. Warrilow (1989), Simulation of the regional climatic impact of Amazon deforestation, *Nature*, *342*(6248), 411–413.

Lewis, S. L., et al. (2009), Increasing carbon storage in intact African tropical forests, *Nature*, *457*(7232), 1003–1006.

Lin, L. I. (1989), A concordance correlation coefficient to evaluate reproducibility, *Biometrics*, *45*(1), 255–268.

Lloyd, J., et al. (2007), An airborne regional carbon balance for Central Amazonia, *Biogeosciences*, *4*(5), 759–768.

Lola da Costa, A. C., et al. (2010), Effect of 7 yr of experimental drought on vegetation dynamics and biomass storage of an eastern Amazonian rainforest, *New Phytol.*, *187*(3), 579–591.

Long, H., L. Vihermaa, S. Waldron, T. Hoey, S. Quemin, and J. Newton (2015), Hydraulics are a first-order control on CO_2 efflux from fluvial systems, *J. Geophys. Res. Biogeosci.*, *120*, 1912–1922, doi:10.1002/2015JG002955.

Lopez-Gonzalez, G., S. L. Lewis, M. Burkitt, and O. L. Phillips (2012), Forest plots database. [Available at www.forestplots.net, Date of extraction 03,02,12.]

Luyssaert, S., et al. (2007), CO_2 balance of boreal, temperate, and tropical forests derived from a global database, *Global Change Biol.*, *13*(12), 2509–2537.

Lyne, V. D., and M. Hollick (1979), Stochastic time-variable rainfall-runoff modelling, paper presented at Hydrology and Water Resources Symposium, Inst. of Eng., Perth, Australia.

Malhi, Y., et al. (2014), The productivity, metabolism and carbon cycle of two lowland tropical forest plots in south-western Amazonia, Peru, *Plant Ecol. Diversity*, *7*(1-2), 85–105.

Marvin, D. C., G. P. Asner, D. E. Knapp, C. B. Anderson, R. E. Martin, F. Sinca, and R. Tupayachi (2014), Amazonian landscapes and the bias in field studies of forest structure and biomass, *Proc. Natl. Acad. Sci. U.S.A.*, doi:10.1073/pnas.1412999111.

Mayorga, E., A. K. Aufdenkampe, C. A. Masiello, A. V. Krusche, J. I. Hedges, P. D. Quay, J. E. Richey, and T. A. Brown (2005), Young organic matter as a source of carbon dioxide outgassing from Amazonian rivers, *Nature*, *436*(7050), 538–541.

McDowell, W. H. (1998), Internal nutrient fluxes in a Puerto Rican rain forest, *J. Trop. Ecol.*, *14*, 521–536.

Mekonnen, G. B., S. Matula, F. Doležal, and J. Fišák (2015), Adjustment to rainfall measurement undercatch with a tippingbucket rain gauge using ground-level manual gauges, *Meteorol. Atmos. Phys.*, *127*, 241–256.

Monteiro, M. T. F., S. M. Oliveira, F. J. Luizao, L. A. Candido, F. Y. Ishida, and J. Tomasella (2014), Dissolved organic carbon concentration and its relationship to electrical conductivity in the waters of a stream in a forested Amazonian blackwater catchment, *Plant Ecol. Diversity*, *7*(1-2), 205–213.

Nepstad, D. C., I. M. Tohver, D. Ray, P. Moutinho, and G. Cardinot (2007), Mortality of large trees and lianas following experimental drought in an Amazon forest, *Ecology*, *88*(9), 2259–2269.

Neu, V., C. Neill, and A. V. Krusche (2011), Gaseous and fluvial carbon export from an Amazon forest watershed, *Biogeochemistry*, *105*(1-3), 133–147.

Öquist, M. G., K. Bishop, A. Grelle, L. Klemedtsson, S. J. Köhler, H. Laudon, A. Lindroth, M. Ottosson-Löfvenius, M. B. Wallin, and M. B. Nilsson (2014), The full annual carbon balance of boreal forests is highly sensitive to precipitation, *Environ. Sci. Technol. Lett.*, *1*, 315–319, doi:10.1021/ez500169j.

Phillips, O. L., et al. (1998), Changes in the carbon balance of tropical forests: Evidence from long-term plots, *Science*, *282*(5388), 439–442.

Phillips, O. L., et al. (2010), Drought-mortality relationships for tropical forests, *New Phytol.*, *187*(3), 631–646.

Pregitzer, K. S., and E. S. Euskirchen (2004), Carbon cycling and storage in world forests: Biome patterns related to forest age, *Global Change Biol.*, *10*(12), 2052–2077.

Quesada, C. A., et al. (2010), Variations in chemical and physical properties of Amazon forest soils in relation to their genesis, *Biogeosciences*, *7*(5), 1515–1541.

Quesada, C. A., J. Lloyd, L. O. Anderson, N. M. Fyllas, M. Schwarz, and C. I. Czimczik (2011), Soils of Amazonia with particular reference to the RAINFOR sites, *Biogeosciences*, *8*(6), 1415–1440.

Rasera, M., M. V. R. Ballester, A. V. Krusche, C. Salimon, L. A. Montebelo, S. R. Alin, R. L. Victoria, and J. E. Richey (2008), Small rivers in the southwestern Amazon and their role in CO_2 outgassing, *Earth Interact.*, *12*, 1–16, doi:10.1175/2008EI257.1.

Rasera, M., A. V. Krusche, J. E. Richey, M. V. R. Ballester, and R. L. Victoria (2013), Spatial and temporal variability of pCO_2 and CO_2 efflux in seven Amazonian Rivers, *Biogeochemistry*, *116*, 241–259.

R Core Team (2014), *R: A Language and Environment for Statistical Computing*, edited, R Foundation for Statistical Computing, Vienna.

Rebsdorf, A., N. Thyssen, and M. Erlandsen (1991), Regional and temporal variation in pH, alkalinity and carbon dioxide in Danish streams, related to soil type and landuse, *Freshwater Biol.*, *25*(3), 419–435.

Restrepo-Coupe, N., et al. (2013), What drives the seasonality of photosynthesis across the Amazon Basin? A cross-site analysis of eddy flux tower measurements from the Brasil flux network, *Agric. For. Meteorol.*, *182*, 128–144.

Richey, J. E., J. M. Melack, A. K. Aufdenkampe, V. M. Ballester, and L. L. Hess (2002), Outgassing from Amazonian rivers and wetlands as a large tropical source of atmospheric CO_2, *Nature*, *416*(6881), 617–620.

Saatchi, S., S. Asefi-Najafabady, Y. Malhi, L. E. O. C. Aragao, L. O. Anderson, R. B. Myneni, and R. Nemani (2013), Persistent effects of a severe drought on Amazonian forest canopy, *Proc. Natl. Acad. Sci. U.S.A.*, *110*(2), 565–570.

Saleska, S., et al. (2003), Carbon in Amazon forests: Unexpected seasonal fluxes and disturbance-induced losses, *Science*, *302*(5650), 1554–1557.

Saleska, S., H. da Rocha, B. Kruijt, and A. Nobre (2009), Ecosystem carbon fluxes and Amazonian Forest metabolism, in *Amazonia and Global Change*, edited by M. Keller et al., pp. 389–407, AGU, Washington, D. C.

Salimon, C., E. dos Santos Sousa, S. R. Alin, A. V. Krusche, and M. V. Ballester (2013), Seasonal variation in dissolved carbon concentrations and fluxes in the upper Purus River, southwestern Amazon, *Biogeochemistry*, *114*(1-3), 245–254.

Saunders, T. J., M. E. McClain, and C. A. Llerena (2006), The biogeochemistry of dissolved nitrogen, phosphorus and organic carbon along terrestrial-aquatic flowpaths of a montane headwater catchment in the Peruvian Amazon, *Hydrol. Processes*, *20*, 2549-2562.

Selva, E. C., E. G. Couto, M. S. Johnson, and J. Lehmann (2007), Litterfall production and fluvial export in headwater catchments of the southern Amazon, *J. Trop. Ecol.*, *23*, 329–335.

Servicio Nacional de Meteorología e Hidrología del Perú (2014), [Available at http://www.senamhi.gob.pe/.]

Shibata, H., H. Mitsuhashi, Y. Miyake, and S. Nakano (2001), Dissolved and particulate carbon dynamics in a cool-temperate forested basin in northern Japan, *Hydrol. Processes*, *15*(10), 1817–1828.

Shukla, J., C. Nobre, and P. Sellers (1990), Amazon deforestation and climate change, *Science*, *247*(4948), 1322–1325.

Sousa, E. S., C. I. Salimon, R. L. Victoria, A. V. Krusche, S. R. Alin, and N. K. Leite (2008), Dissolved inorganic carbon and pCO_2 in two small streams draining different soil types in southwestern Amazonia, Brazil, *Rev. Ambiente Água*, *3*(2), 37–50.

Stoy, P. C., G. G. Katul, M. B. S. Siqueira, J.-Y. Juang, K. A. Novick, J. M. Uebelherr, and R. Oren (2006), An evaluation of models for partitioning eddy covariance-measured net ecosystem exchange into photosynthesis and respiration, *Agric. For. Meteorol.*, *141*, 2–18.

Townsend-Small, A., J. L. Noguera, M. E. McClain, and J. A. Brandes (2007), Radiocarbon and stable isotope geochemistry of organic matter in the Amazon headwaters, Peruvian Andes, *Global Biogeochem. Cycles*, *21*, GB2029, doi:10.1029/2006GB002835.

Townsend-Small, A., M. E. McClain, B. Hall, J. L. Noguera, C. A. Llerena, and J. A. Brandes (2008), Suspended sediments and organic matter in mountain headwaters of the Amazon River: Results from a 1-year time series study in the central Peruvian Andes, *Geochim. Cosmochim. Acta*, *72*(3), 732–740.

van Buuren, S., and K. Groothuis-Oudshoorn (2011), MICE: Multivariate Imputation by Chained Equations in R, *J. Stat. Software*, *45*(3), 1–67.

Vihermaa, L. E., S. Waldron, M. H. Garnett, and J. Newton (2014), Old carbon contributes to aquatic emissions of carbon dioxide in the Amazon, *Biogeosciences*, *11*, 3635–3645.

Waldron, S., E. M. Scott, and C. Soulsby (2007), Stable isotope analysis reveals lower-order river dissolved inorganic carbon pools are highly dynamic, *Environ. Sci. Technol.*, *41*(17), 6156–6162.

Waldron, S., E. M. Scott, L. E. Vihermaa, and J. Newton (2014), Quantifying precision and accuracy of measurements of dissolved inorganic carbon stable isotopic composition using continuous-flow isotope-ratio mass spectrometry, *Rapid Commun. Mass Spectrom.*, *28*(10), 1117–1126.

Waterloo, M. J., et al. (2006), Export of organic carbon in run-off from an Amazonian rainforest blackwater catchment, *Hydrol. Processes*, *20*(12), 2581–2597.

Weatherbase (2015), Weather Tambopata, Peru. [Available at http://www.weatherbase.com/weather/weather.php3?s=604579&cityname=Tambopata-Madre-de-Dios.]

Werth, D., and R. Avissar (2002), The local and global effects of Amazon deforestation, *J. Geophys. Res.*, *107*(D20), 8087, doi:10.1029/2001JD000717.

Zanchi, F. B., M. J. Waterloo, A. Peralta Tapia, M. S. Alvarado Barrientos, M. A. Bolson, F. J. Luizão, A. O. Manzi, and A. J. Dolman (2015), Water balance, nutrient and carbon export from a heath forest catchment in central Amazonia, Brazil, *Hydrol. Processes*, doi:10.1002/hyp.10458.

Zeri, M., L. D. A. Sa, A. O. Manzi, A. C. Araujo, R. G. Aguiar, C. von Randow, G. Sampaio, F. L. Cardoso, and C. A. Nobre (2014), Variability of carbon and water fluxes following climate extremes over a tropical forest in southwestern Amazonia, *PLoS One*, *9*(2), e88130.